

Damping and Transfer Control of Liquid in a Cylindrical Container Using a Wheeled Mobile Robot

Masafumi Hamaguchi and Takao Taniguchi

*Department of Electronic and Control Systems Engineering
Shimane University*

1060 Nishikawatsu, Matsue, Shimane, 690-8504 Japan

Email: hamaguchi@ecs.shimane-u.ac.jp

Abstract—A spherical pendulum-type model is constructed to represent liquid sloshing in a cylindrical container, caused by the motions of a wheeled mobile robot (WMR). The model is used to design a path and an acceleration pattern for the WMR in consideration of the damping of sloshing in the container. The curvature radius of the path and the acceleration pattern of the WMR are determined using an input shaping method. A PD controller is used so that the WMR can trace the designed path. Maximum displacement magnitude of the sloshing is considered as a constraint condition in this control transfer system. The effectiveness of the present method is clarified through simulations and experiments.

Keywords—Transfer control, Sloshing, Damping control, Wheeled mobile robot, Path design

I. INTRODUCTION

With the advancement of automation at various factories, liquid container transfers have become very important processes in the production line. For example, there are transfers of molten metals, transfers of molds after pouring as part of material processing in steel and casting industries, or transfers of raw material solutions and mixed solutions in chemical plants without using pipes. In such processes, containers have generally no lid to speed up and simplify pouring works. In liquid container transfers, sloshing (liquid vibration) is generated by changes in the container's acceleration. Overflows and the degradation of quality caused by sloshing in containers are problems that directly affect productivity. For instance, there is the degradation by the contamination of air and slag in transfers of molten metals.

One of authors previously reported a transfer control system involving a rectangular container on a cart along a straight path [1], [2]. In actual processes, transfer paths often include curved sections, and cylindrical containers are also usually used. In a curved path transfer using a cylindrical container, a swirling phenomenon or rotary sloshing is sometimes observed. One of authors developed a model of sloshing and a two-degree-of-freedom control system in a cylindrical container transfer along a curved path [3]. By using only the container velocity control, lateral sloshing was not damped. We demonstrated that lateral sloshing could be damped by the path design using an input shaping method [4]. In the studies

mentioned above, it was considered that the liquid container was transferred with the cart along fixed paths or rails. Such transfer systems cannot provide the most effective use of the factory space, because the space is occupied by the fixed paths. In addition, this method does not allow flexibly to adapt to changes in processes. The transfer system using wheeled mobile robots (WMRs) is one solution to these problems.

Liquid container transfer using robot arms, cart or vehicles are studied [5]–[7]. In those papers, damping the sloshing is discussed though, damping path design and trace control are not considered. Though path planning and trace control for WMRs have been studied [8], [9], the study on the liquid container transfer using WMR is not seen.

This paper describes a velocity control, a path design and a trace control for WMR to damp the sloshing in a cylindrical container transfer. Damping effect on sloshing and traceability of WMR are demonstrated by means of simulations and experiments.

II. EXPERIMENTAL EQUIPMENT

The liquid in the cylindrical container is transferred with the WMR as shown in Fig. 1. The WMR is the tricycle type which consists of two driving wheels and one steering wheel. These wheels are driven by DC motors. The rotational speed of the right and left driving wheels are measured by means of rotary encoders, and the steering angle is done by the potentiometer. The steering angle is adjusted using a PID controller in order to work as a caster. This steering system improves straightness and steering above those of common casters. The driving wheels are driven using a PID controller to obtain the desired speed.

The container is mounted on the WMR. The inner diameter of the container is 0.10 m, its height is 0.30 m. Water is chosen as the target liquid because of its simplicity of handling and low cost. Two laser displacement sensors are used to observe the liquid level at the front measuring point and the left side one. The water is colored with a white paint so that the laser sensors can detect the water surface.

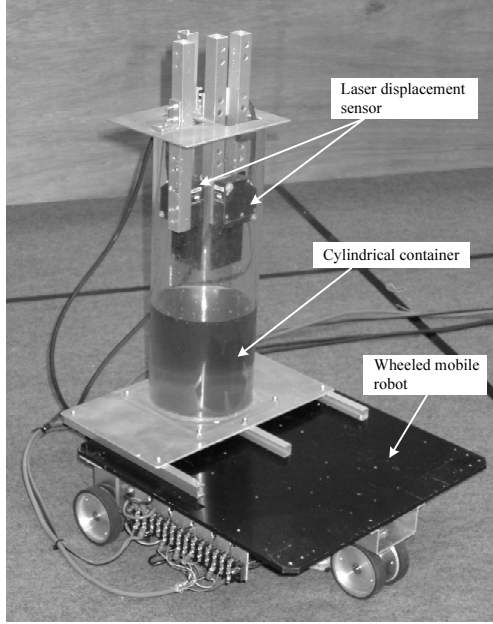


Fig. 1. Experimental equipment

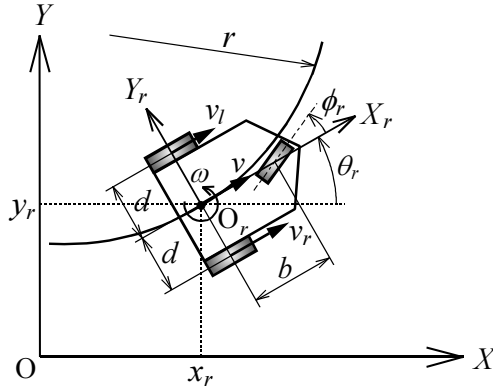


Fig. 2. A schematic representation of the WMR

III. MODEL EQUATIONS

The model equations of the WMR and of sloshing are described for the design of a transfer control system. When the mass of the container with the liquid is sufficiently heavier than that of the WMR, pitching and rolling motions can be considered as the model equations of the WMR and sloshing. The terms of these motions, here, are omitted from the model equations.

A. Wheeled Mobile Robot

A schematic representation of the WMR is shown in Fig. 2. Disregarding slipping of the wheels, the kinematic model

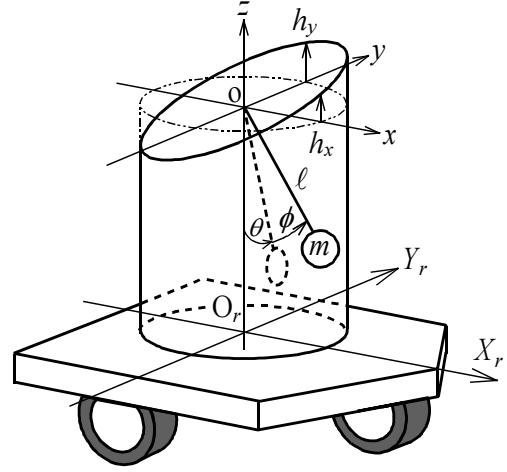


Fig. 3. Spherical pendulum-type sloshing model

equations of the WMR are shown as follows:

$$\dot{x}_r = v \cos \theta_r, \quad \dot{y}_r = v \sin \theta_r, \quad \dot{\theta}_r = \omega, \quad (1)$$

$$v = \frac{v_r + v_l}{2}, \quad \omega = \frac{v_r - v_l}{2d}, \quad (2)$$

$$\tan \phi_r = \frac{b}{r}, \quad r = \frac{v}{\omega}, \quad (3)$$

where x_r and y_r are the positions of the axle center O_r on X - Y plane, v is the velocity of the axle center O_r , θ_r is the direction of the WMR, ω is the angular velocity of the WMR around the vertical axis, v_r and v_l are the circumferential speeds of the wheels of right and left, respectively, $2d$ is the distance between driving wheels, b is the wheelbase, ϕ_r is the steering angle, and r is the curvature radius of the path. The position x_r , y_r and the direction θ_r are determined by the circumferential speeds of the right and left wheels, v_r and v_l . These values of v_l , v_r and ϕ_r are controlled with appropriate PID controllers. Assuming that the time constant of the WMR is sufficiently decreased with these controllers, here, the dynamics of the WMR is disregarded.

The model equations of the driving wheels are given as a first-order delay system:

$$\left. \begin{aligned} \dot{v}_r &= -\frac{1}{T_w} v_r + \frac{K_w}{T_w} u_r, \\ \dot{v}_l &= -\frac{1}{T_w} v_l + \frac{K_w}{T_w} u_l, \end{aligned} \right\} \quad (4)$$

where u_r and u_l are the input voltages to the wheels of right and left, respectively, T_w is the time constant, and K_w is the gain.

B. Sloshing

The spherical pendulum-type sloshing model [3] is shown in Fig. 3. The sloshing model approximately expresses (1, 1)-mode sloshing, which is a dominant mode of sloshing in the case of container transfer without intense vibrations. In this model, the liquid surface is considered to be the plane

perpendicularly installed on the pendulum. That is to say, the sloshing has been replaced with the motion of the pendulum. Using the Newton-Euler method, the equations of the sloshing model are obtained as follows:

$$\left. \begin{aligned} \ddot{\theta} &= -\frac{g \sin \theta}{\ell \cos \phi} + 2\dot{\theta}\dot{\phi} \tan \phi + 2\dot{\phi} \frac{v}{r} \cos \theta \\ &+ \frac{v^2}{r^2} \sin \theta \cos \theta - \frac{c_\theta}{m} \dot{\theta} \cos^2 \theta \\ &+ \frac{c_\phi}{m} \dot{\phi} \sin \theta \cos \theta \tan \phi \\ &+ \dot{v} \cos \theta \left(\frac{\tan \phi}{r} - \frac{1}{\ell \cos \phi} \right), \\ \ddot{\phi} &= -\frac{g \sin \phi}{\ell \cos \theta} + 2\dot{\theta}\dot{\phi} \tan \theta \sin^2 \phi \\ &- 2\dot{\theta} \frac{v}{r} \cos \theta \cos^2 \phi - \frac{v^2}{\ell r} \cos \phi \\ &+ 2\dot{\phi} \frac{v}{r} \sin \theta \sin \phi \cos \phi \\ &+ \left(\frac{v^2}{r^2} - \dot{\theta}^2 \right) \sin \phi \cos \phi \\ &- \frac{c_\theta}{m} \dot{\phi} \cos^2 \phi - \frac{\dot{v}}{r} \sin \theta \cos^2 \phi \\ &- \ddot{\theta} \tan \theta \sin \phi \cos \phi, \end{aligned} \right\} \quad (5)$$

where θ is the angle of the pendulum mapped onto the z-x plane, ϕ is the angle between the original pendulum and the mapped pendulum, g is the gravitational acceleration, ℓ is the equivalent length of the pendulum, m is the mass of the liquid, and c_θ and c_ϕ are the equivalent coefficients of viscosity for sloshing on θ and ϕ , respectively. The displacement of the liquid level h_x at the front measuring point and h_y at the left side measuring point are described as

$$h_x = L \tan \theta, \quad h_y = \frac{L \tan \phi}{\cos \theta}, \quad (6)$$

where L is the distance between the measuring point and the center of the container.

Equations (5) and (6) are linearized by using a linear approximation technique at $\theta \approx 0$ and $\phi \approx 0$ in order to create a linear control system, because the above nonlinear model is too complicated to allow for the design of a control system. The coupling terms of θ and ϕ are neglected here. The linearized equations are as follows:

$$\left. \begin{aligned} \ddot{\theta} &= -\frac{g}{\ell} \theta - \frac{c_\theta}{m} \dot{\theta} - \frac{\dot{v}}{\ell} + \frac{1}{r} \left(2v\dot{\phi} + \frac{v^2 \theta}{r} + \dot{v}\phi \right), \\ \ddot{\phi} &= -\left(\frac{g}{\ell} - \frac{v^2}{r^2} \right) \phi - \frac{c_\phi}{m} \dot{\phi} - \frac{v^2}{\ell r} - \frac{1}{r} (2v\dot{\theta} + \dot{v}\theta), \\ h_x &= L\theta, \quad h_y = L\phi. \end{aligned} \right\} \quad (7)$$

$$h_x = L\theta, \quad h_y = L\phi. \quad (8)$$

IV. ASSUMPTIONS AND PROBLEM STATEMENT

Followings are assumed:

- Transfer paths consist of straight paths, curved paths of circular arcs and transition paths between them.

- Transfer velocity v_s is fixed on curved paths and sloshing is completely damped at starting points of curved paths.
- Acceleration and deceleration of a WMR are carried out only on straight paths.
- Start and goal points exist on straight paths.

These assumptions are introduced to design easily the transfer control system. It is also easy to realize these assumptions.

The transfer control system to damp the sloshing in the container is constructed under these assumptions. The control system is realized using the velocity control and the path design for the WMR. Under these assumptions, the acceleration change for θ is generated only on the straight path with $r = \infty$, and that for ϕ is done when $\theta = \dot{\theta} = 0$. Therefore, the linearized sloshing model (7) and (8) are modified as follows:

$$\ddot{\theta} = -\frac{g}{\ell} \theta - \frac{c_\theta}{m} \dot{\theta} - \frac{1}{\ell} \alpha_{X_r}, \quad h_x = L\theta, \quad (9)$$

$$\ddot{\phi} = -\left(\frac{g}{\ell} - \frac{v^2}{r^2} \right) \phi - \frac{c_\phi}{m} \dot{\phi} - \frac{1}{\ell} \alpha_{Y_r}, \quad h_y = L\phi, \quad (10)$$

where $\alpha_{X_r} = \dot{v}$ is the running acceleration on X_r -axis, and $\alpha_{Y_r} = v^2/r$ is the centripetal acceleration on Y_r -axis. Equation (9) is used for the velocity control, and (10) is employed in the design of the transfer path.

V. TRANSFER CONTROL SYSTEM

The transfer control system is constructed as an open loop control system without employing sensor feedback to monitor the sloshing. The open loop control system is excellent in terms of cost, when modeling errors and disturbances can be neglected. Many sensors and high-performance computers are required in feedback control systems.

An input shaping method are adopted for the velocity control and the path design of the WMR.

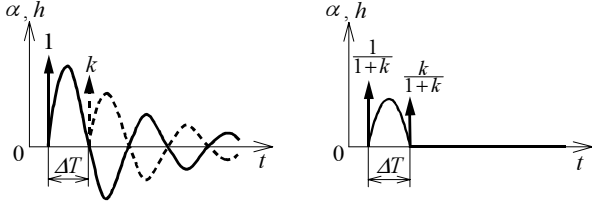
A. Input Shaping Method

An input shaping method [10] is adopted for the transfer control system. The principle of the two-impulse input technique is illustrated in Fig. 4. The vibration caused by the unit impulse input of the acceleration is canceled by another impulse input that has an amplitude of k and a time delay of ΔT . When the transfer function is a linear second-order system given as (11), ΔT and k can be analytically formulated as (12) [10].

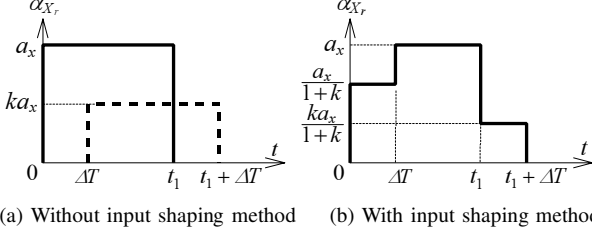
$$G(s) = \frac{K\omega_n^2}{s^2 + 2\zeta\omega_n s + \omega_n^2}, \quad (11)$$

$$\Delta T = \frac{\pi}{\omega_n \sqrt{1 - \zeta^2}}, \quad k = \exp\left(\frac{-\zeta\pi}{\omega_n \sqrt{1 - \zeta^2}} \right), \quad (12)$$

where ω_n is the system's natural angular frequency, ζ is the damping ratio, and K is the gain.



(a) Response without the method (b) Response with the method
Fig. 4. Two-impulse input technique in input shaping method



(a) Without input shaping method (b) With input shaping method
Fig. 5. Running acceleration pattern using the input shaping method to damp the sloshing

B. Velocity Control

From (9), the transfer function from the running acceleration α_{x_r} to the displacement of the liquid level h_x at the front measuring point is the same form as (11), where the coefficients are as follows:

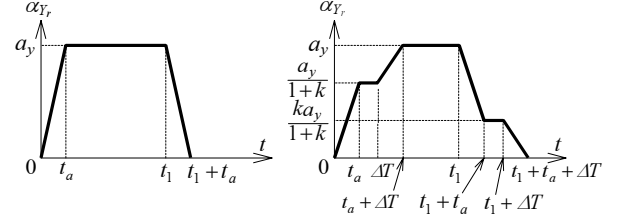
$$\omega_n = \sqrt{\frac{g}{\ell}}, \quad \zeta = \frac{c\theta}{2m} \sqrt{\frac{\ell}{g}}, \quad K = -\frac{L}{g}. \quad (13)$$

The running acceleration pattern of the WMR can be shaped using the input shaping method to damp the sloshing. The solid line shown in Fig. 5(a) is the acceleration pattern for the trapezoidal velocity pattern, where a_x is the maximum value of the acceleration, t_1 is the acceleration time, and $a_x t_1$ gives the transfer velocity v_s . The acceleration pattern shown with the dashed line cancels the sloshing generated by that shown with the solid line. The parameter values of ΔT and k are calculated using (12). The deceleration pattern is similar to this. The liquid container transfer without residual sloshing is realized controlling the velocity of the WMR in order to conform to the acceleration pattern shown in Fig. 5(b).

C. Path Design

In the present velocity control, it is impossible to control the displacement of the liquid level h_y directly. The displacement h_y is not controllable by the running acceleration α_{x_r} , as it is clear in (10). In order to damp the displacement h_y , the curvature radius r of the path is designed by using the input shaping method.

From (10), the transfer function from the centripetal acceleration α_{y_r} to the displacement of the liquid level h_y is the same form as (11). The parameter values of the input shaping method, therefore, are calculated using (12). Fig. 6 shows the centripetal acceleration pattern to damp the displacement h_y .



(a) Without input shaping method (b) With input shaping method
Fig. 6. Centripetal acceleration pattern using the input shaping method to damp the sloshing

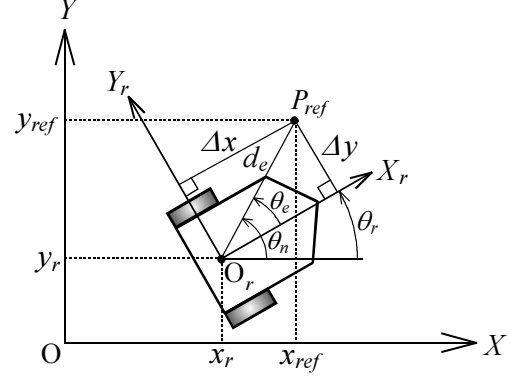


Fig. 7. Position error for reference position

Fig. 6(a) shows the centripetal acceleration pattern on the curved path of the constant curvature radius r_s , where a_y is the maximum value of the acceleration, t_a is the transition time for steering, and t_1 denotes the running time on the curved path as $t_a = 0$. The values of t_a and t_1 are obtained by

$$t_a = \frac{dv_s}{r_s a_x}, \quad t_1 = \frac{r_s \theta_{ref}}{v_s}, \quad (14)$$

where θ_{ref} is the desired turning angle of the WMR at the endpoint of the curved path. Fig. 6(b) shows the centripetal acceleration pattern necessary to damp the sloshing, and this pattern is realized by calculating the reference curvature radius of the path on $\alpha_{y_r} = v_s^2/r$.

D. Trace Control

The reference acceleration patterns of the driving wheels, \ddot{v}_r and \ddot{v}_l , are determined from Fig. 5 and 6 using (2) and (3). Then, the reference input voltages to the wheels, u_{pr} and u_{pl} , are calculated using (4). The position error for the designed path may occur only by applying the voltages, u_{pr} and u_{pl} , to the WMR, because there are modeling errors in (4) and slipping of the wheels. To improve the traceability for the designed path, a PD controller is introduced.

Fig. 7 shows a position error for a reference position. The distance d_e between the axle center O_r and the reference point

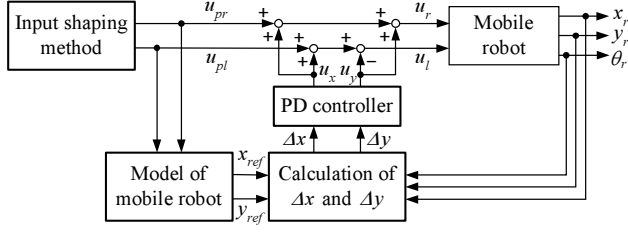


Fig. 8. Trace control system with PD controller

P_{ref} and the angle θ_n are given as follows:

$$d_e = \sqrt{(x_{ref} - x_r)^2 + (y_{ref} - y_r)^2}, \quad (15)$$

$$\theta_n = \tan^{-1} \frac{y_{ref} - y_r}{x_{ref} - x_r}, \quad (16)$$

where x_{ref} and y_{ref} are the positions of P_{ref} on X-axis and Y-axis, respectively. The position errors Δx and Δy on X_r-axis and Y_r-axis, respectively, are given as

$$\Delta x = d_e \cos \theta_e, \quad \Delta y = d_e \sin \theta_e, \quad (17)$$

$$\theta_e = \theta_n - \theta_r. \quad (18)$$

Using PD controller, correctional inputs u_x and u_y are obtained as follows:

$$\left. \begin{aligned} u_x &= K_p \Delta x + K_d \Delta \dot{x}, \\ u_y &= K_p \Delta y + K_d \Delta \dot{y}, \end{aligned} \right\} \quad (19)$$

where K_p and K_d are the control gains. Therefore, the final control inputs u_r and u_l are given as

$$\left. \begin{aligned} u_r &= u_{pr} + u_x + u_y, \\ u_l &= u_{pl} + u_x - u_y. \end{aligned} \right\} \quad (20)$$

The sign of u_y is different between u_r and u_l to turn to the reference point. The trace control system is shown in Fig. 8. This control system is a kind of 2-degree-freedom control system (model following control system). The part of the input shaping method is a feedforward controller and the PD controller is a feedback controller.

VI. RESULTS

Values of the parameters used in the experiments are shown in Table I. In the experimental condition, the term of v^2/r^2 in (10) is unconsidered because the value of v^2/r^2 is sufficiently smaller than that of g/ℓ . The reference transfer path shown in Fig. 9 consists of three sections: a straight path of 2.0 m, a quarter circle of 0.5 m radius, and a straight path of 1.2 m. The geometric form of the pass is decided considering the layout of the factory or the production line. The reference path in Fig. 9 is an example. In practice, the reference path has allowance in width. The reference path, therefore, means the nominal path.

The designed and nondesigned paths deviate from the goal. This is the reason why the transition time t_a is only

TABLE I
VALUES OF PARAMETERS USED IN EXPERIMENTS

wheelbase	b	0.24 m
distance between driving wheels	$2d$	0.240 m
time constant of driving wheel	T_w	0.517 s
gain of driving wheel	K_w	0.262 m/(sV)
distance of measuring point	L	0.025 m
static liquid level	h_s	0.125 m
length of pendulum	ℓ	0.0272 m
mass of liquid	m	0.982 kg
coefficients of viscosity	c_θ, c_ϕ	0.915 Ns/m
maximum acceleration	a_x	0.625 m/s ²
transfer velocity	v_s	0.5 m/s
curvature radius	r_s	0.5 m
desired turning angle	θ_{ref}	$\pi/2$ rad
time delay	ΔT	0.1654 s
amplitude	k	0.924
control gain	K_p	0.5
control gain	K_d	5.0

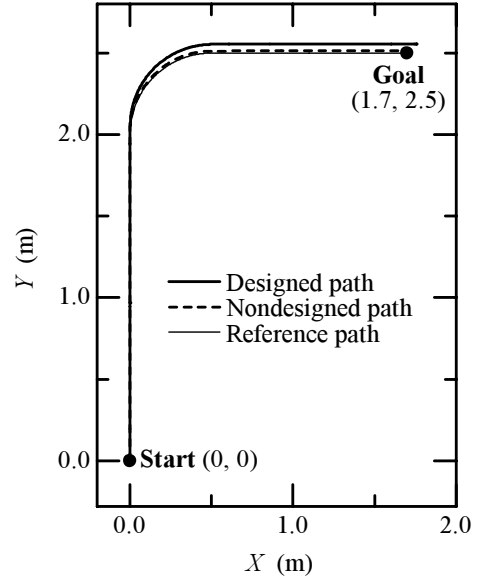


Fig. 9. Designed path

considered in the nondesigned path, and both the transition time t_a and the time delay ΔT are considered in the designed path. Here, lengths of two straight sections in both paths are set to be 2.0 m and 1.2 m, respectively. Namely, the nondesigned path and the designed path correspond to Fig. 6(a) and (b), respectively. When the differences at the goal position between the designed path and the reference are named ΔX on the X-axis and ΔY on the Y-axis, lengths of straight sections can be easily adjusted by using ΔX and ΔY to agree with the goal position. The values of ΔX and ΔY are evaluated from the simulation results in which the accelerating patterns of Fig. 5 and 6 are applied to the models of (2) and (3). The designed path with the adjustment is shown in Fig. 10. It is confirmed that the designed path agrees almost with the reference path. The maximum error

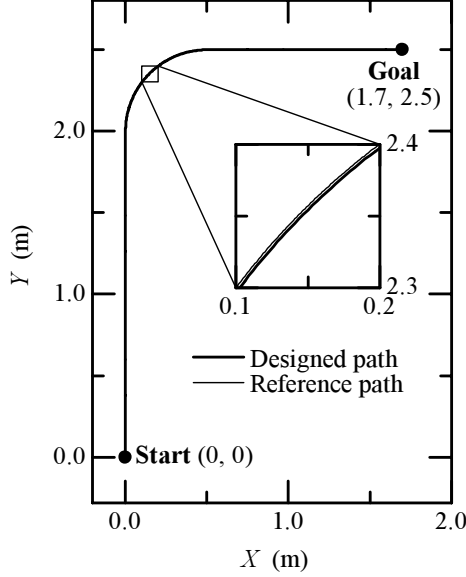


Fig. 10. Designed path with adjustment

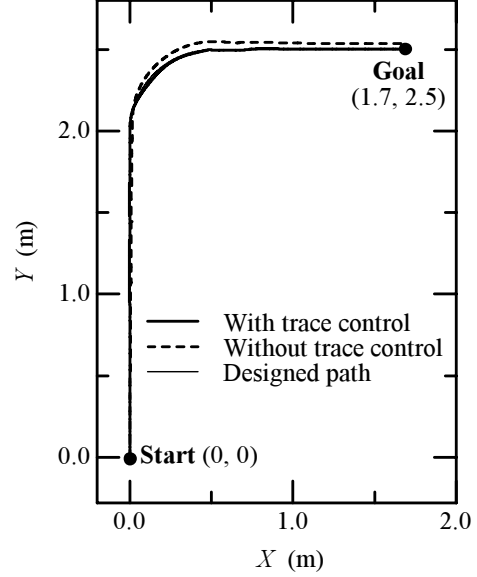


Fig. 12. Trajectory of WMR in experimental result of transfer control

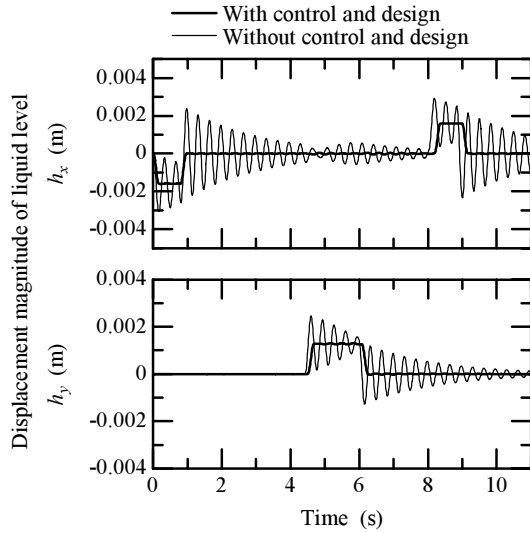


Fig. 11. Simulation results of transfer control applied to nonlinear sloshing model

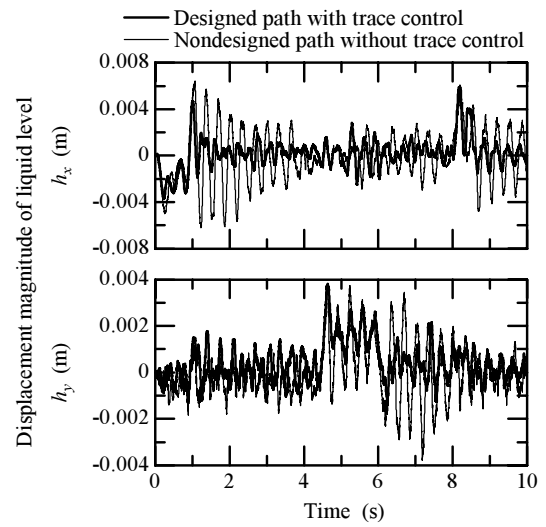


Fig. 13. Displacement magnitude of liquid level in experimental result of transfer control

between the designed path and the reference path is 0.0021m on curved section, that is, the relative error for the radius is only 0.42%.

Fig. 11 shows the simulation results of the transfer control using the input shaping method. The obtained accelerating pattern is applied to the models of (1), (3) and (5) using the Runge Kutta method with a 1.0 ms sampling time. With respect to h_x and h_y , there is a little residual vibration. Results of applying to the linear sloshing models of (9) and (10) have no residual vibration.

The experimental results of the transfer control considering the damping of sloshing and the traceability for the designed path are shown in Fig. 12 and 13. Therefore, sufficient

traceability and damping effect are obtained by using the trace control system.

A constraint condition to the maximum displacement magnitude of liquid level h_{max} should be introduced in the present transfer system. If it is assumed that the accelerations α_x and α_y are constant, the maximum displacement magnitude of liquid level h_{xmax} and h_{ymax} are obtained by substituting $\dot{\theta} = \ddot{\theta} = \dot{\phi} = \ddot{\phi} = 0$ in (9) and (10). The maximum values of α_x and α_y are named a_x and a_y , respectively, in Fig. 5 and 6. The h_{xmax} and h_{ymax} are calculated as follows:

$$h_{xmax} = L \frac{a_x}{g}, \quad h_{ymax} = L \frac{a_y}{g}, \quad (21)$$

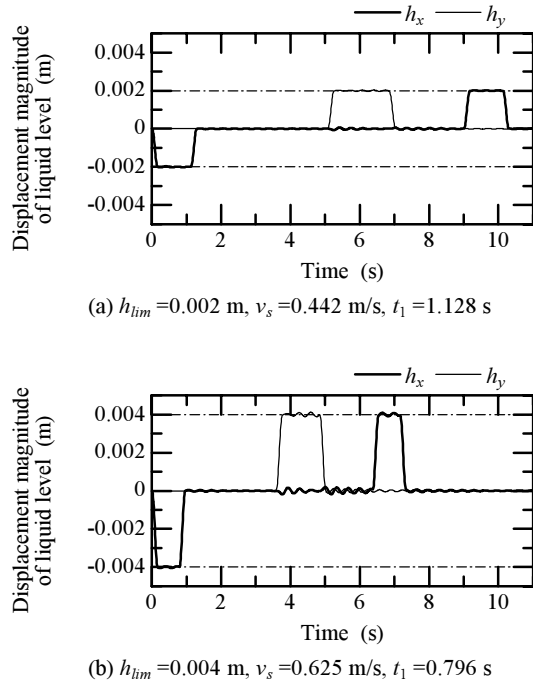


Fig. 14. Simulation results of velocity control and path design considering constraint conditions

where $a_x = v_s/t_1$, $a_y = v_s^2/r_s$, and the term of v^2/r^2 in (10) is neglected. When the limitation of the maximum displacement magnitude of liquid level h_{lim} is given, the transfer velocity v_s and the accelerating time t_1 are obtained as follows:

$$v_s \leq \sqrt{\frac{r_s h_{lim} g}{L}}, \quad t_1 \geq \frac{v_s L}{h_{lim} g}, \quad (22)$$

where the distance of measuring point L , the curvature radius of the path r_s and the length of the pendulum ℓ are given as the specifications by users.

The simulation results of transfer control with constraint conditions for h_{lim} are shown in Fig. 14 and 15. Fig. 14(a) is the result for h_{lim} of 0.002 m, Fig. 14(b) is that for h_{lim} of 0.004 m, where L is 0.05 m of radius of the container. Fig. 15 shows the designed paths that are adjusted to agree with the goal position. It is confirmed that the designed paths are almost never different from the reference path.

VII. CONCLUSION

In this paper, a simplified sloshing model has been constructed using a spherical pendulum. A velocity control and path design to damp the sloshing have been designed by means of an input shaping method for application in a linear sloshing model. The velocity control has been realized by employing a very simple running acceleration pattern, and the designed path is very similar to the reference path. A trace control for the designed path has been attained using a PD controller. The constraint condition for the maximum displacement magnitude of sloshing has been easily considered in the proposed method. It is notable that the proposed

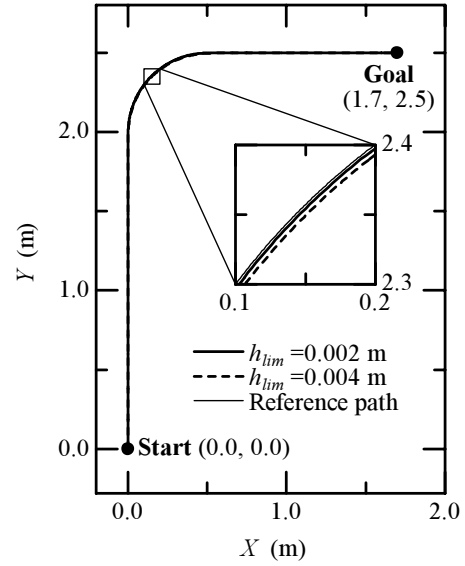


Fig. 15. Designed path of Fig. 14

transfer control system can be constructed with an open loop control for sloshing and has a sufficient damping effect to control sloshing.

If disturbances and modeling errors are critical problems, a control system should have a feedback or a closed loop controller for sloshing. The feedback control for sloshing can improve a damping performance on sloshing.

REFERENCES

- [1] M. Hamaguchi and K. Terashima, "Modeling and Optimal Control of Liquid Vibration in Transferring a Rectangular Container", Proceedings of the FLUCOME, Vol. 1, pp. 379-384, 1994.
- [2] K. Yano, T. Yoshida, M. Hamaguchi and K. Terashima, "Liquid Container Transfer Considering the Suppression of Sloshing for the Change of Liquid Level", Proceedings of the 13th World Congress of IFAC, Vol. B, pp. 193-198, 1996.
- [3] M. Hamaguchi, M. Yamamoto and K. Terashima, "Modeling and Control of Sloshing with Swirling in a Cylindrical Container during a Curved Path Transfer", Proceedings of the 2nd Asian Control Conference, Vol. I, pp. 233-236, 1997.
- [4] M. Hamaguchi and T. Taniguchi, "Transfer Control and Curved Path Design for Cylindrical Liquid Container", Proceedings of the 15th World Congress of IFAC, July, 2002.
- [5] J. T. Feddema, C. R. Dohrmann et al., "Control for Slosh-Free Motion of an Open Container", IEEE Control Systems Magazine, Vol. 17, No. 1, pp. 29-36, 1997.
- [6] K. Yano, T. Toda and K. Terashima, "Sloshing Suppression Control of Automatic Pouring Robot by Hybrid Shape Approach", Proceedings of the 40th IEEE Conference on Decision and Control, Vol. 2, pp. 1328-1333, 2001.
- [7] T. Acarman and U. Ozquner, "Rollover Prevention for Heavy Trucks Using Frequency Shaped Sliding Mode Control", Proceedings of 2003 IEEE Conference on Control Applications, Vol. 1, pp. 7-12, 2003.
- [8] W. Wu, H. Chen and P. Woo, "Time Optimal Path Planning for a Wheeled Mobile Robot", Journal of Robotic Systems, Vol. 17, No. 11, pp. 585-591, 2000.
- [9] M. L. Corradini and G. Orlando, "Robust Tracking Control of Mobile Robots in the Presence of Uncertainties in the Dynamical Model", Journal of Robotic Systems, Vol. 18, No. 6, pp. 317-323, 2001.
- [10] N. C. Singer and W. P. Seering, "Preshaping Command Inputs to Reduce System Vibration", ASME Journal of Dynamic Systems, Measurement, and Control, Vol. 112, pp. 76-82, 1990.